Facile and selective polynitrations at the 4-pyrazolyl dual backbone: A straightforward access to a series of high-density energetic materials

Journal:	*New Journal of Chemistry*
Manuscript ID	NJ-ART-10-2018-005266.R1
Article Type:	Paper
Date Submitted by the Author:	05-Dec-2018
Complete List of Authors:	Domasevitch, Konstantin; National Taras Shevchenko University of Kyiv, Inorganic Chemistry Gospodinov, Ivan; LMU Munich, Chemistry Krautscheid, Harald; Universitaet Leipzig, Anorganische Chemie Klapoetke, Thomas; LMU München, Chemistry Stierstorfer, Joerg; LMU Munich, Chemistry

Journal Name

ARTICLE

Facile and selective polynitrations at the 4-pyrazolyl dual backbone: A straightforward access to a series of high-density energetic materials

Received 00th January 20xx,
Accepted 00th January 20xx

DOI: 10.1039/x0xx00000x

www.rsc.org/

Kostiantyn V. Domasevitch,*[a] Ivan Gospodinov,[b] Harald Krautscheid,[c] Thomas M. Klapötke*[b] and Jörg Stierstorfer[b]

Nitro-functionalized energetic materials are still needed to meet new safety, performance and chemical accessibility demands. The problem of multiple C-nitrations on N-containing heterocycles was resolved successfully for the 4,4′-bipyrazole scaffold. A progression of gradually functionalized 3-nitro-4,4′-bipyrazole (**2**), 3,3′-dinitro-4,4′-bipyrazole (**3**), 3,5-dinitro-4,4′-bipyrazole (**4**), 3,3′,5-trinitro-4,4′-bipyrazole (**5**) and 3,3′,5,5′-tetranitro-4,4′-bipyrazole (**6**) was obtained in excellent yields by highly selective direct nitrations of 4,4′-bipyrazole (**1**). All synthesized polynitro derivatives **3**–**6** exhibit high decomposition temperatures of above 290 °C. The introduction of three (**5**) and four nitro groups (**6**) into the 4,4′-bipyrazole scaffold yields insensitive and thermally stable high explosives with excellent densities and detonation properties. The anhydrous structures of compounds **2**–**6** were obtained by low-temperature XRD. In addition, the performance of compounds **5** and **6** was investigated with the small scale shock reactivity test.

Introduction

Practical uses of high energy density materials, in particular those based on common explosophore nitro groups, imply needs for performance in a combination with thermal stability and insensitivity toward external stimuli.[1] Environmental benign energetic materials, either in the view of green decomposition products or safety of production and storage, is also recognized as an important limitation.[2] The development of such materials is an ongoing challenge since many of the above issues are inherently hardly compatible and the compounds, which fulfill the sensitivity, stability, and performance requirements are still rare.[1] Recent years indicate an enormous interest toward design of such materials, while utilizing polynitrogen heterocycle platforms for accommodation of multiple explosophore groups.[3] In this respect, the nitro-functionalized pyrazole backbone offers many special and valuable possibilities, with such key inputs as high nitrogen content, good thermal stability, chemical robustness and versatility of structural functions due to original protolytic behavior. The prototypical 3,4,5-trinitropyrazole reveals detonation velocity comparable to RDX and HMX and impact sensitivity value close to TNT,[4] while 3,4-dinitropyrazole could be used as a melt-castable explosive, alternatively to TNT.[5] Rapid extension of the nitropyrazole family provided further attractive examples of N-functionalized and N,N′-bridged compounds,[6] bis-pyrazoles,[7,8a] ring-fused systems,[8] amino-, nitramino- and other derivatives[9] used also for production of energetic ionic nitropyrazolates,[1a,10] MOFs,[11] molecular co-crystals[12] and eutectics.[13]

In spite of the satisfactory and promising properties of nitropyrazole materials, their practical impact is still limited in the view of typically insufficient synthetic protocols. All-carbon-nitrated pyrazoles are inaccessible by direct reaction since the initial electrophilic substitution at the 4-position of the ring totally inactivates the substrate.[14] Thus the accumulation of multiple nitro-functions at the pyrazole platform claims for a cascade of sequential reactions, such as *N*-nitrations and thermal rearrangements to 3-nitropyrazoles,[15] oxidation, diazotization, and direct nitration, which have been involved towards the syntheses of any of the highly substituted species, such as 3,4,5-trinitropyrazole,[3,4] 4,4′,5,5′-tetranitro-3,3′-bipyrazole,[7b] etc. (Fig. 1).

In the present study, we introduce a paradigm resolving these disadvantages, while providing direct access to a series of high-density polynitropyrazole

[a] *Inorganic Chemistry Department, Taras Shevchenko National University of Kyiv, Volodymyrska Str. 64/13, Kyiv 01601, Ukraine. E-mail: dk@univ.kiev.ua*
[b] *Ludwig-Maximilian University Munich, Department of Chemistry, Butenandtstr. 5-13 (D), 81377 München, Germany. E-mail: tmk@cup.uni-muenchen.de Homepage: http://www.hedm.cup.uni-muenchen.de*
[c] *Institut für Anorganische Chemie, Universität Leipzig, Johannisallee 29, D-04103 Leipzig, Germany.*

† Footnotes relating to the title and/or authors should appear here.
Includes experimental details, crystallographic data (CCDC: 1836403-1836408) and detailed description of crystal structures, theoretical calculation, thermal stability data and NMR spectra. See DOI: 10.1039/x0xx00000x

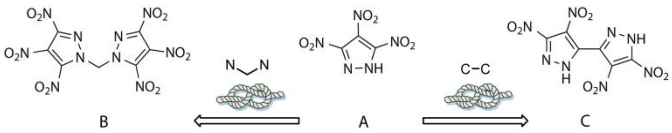

Fig 1. Controlling the energetic properties via hypothetical link-up of nitro-pyrazoles based energetic materials: A) 3,4,5-trinitropyrazole; B) bis(3,4,5-trinitropyrazolyl) methane; C) 4,4′,5,5′-tetranitro-3,3′-bipyrazole.

compounds 2–6 by very simple procedures, which do not extend beyond common nitration in mixed acid. Coupling of two pyrazole rings, with a mutual interlock of reactive 4,4′-positions, is a key prerequisite for subsequent easy substitution at every of the four *C*3(5)-positions left. Therefore, the system is especially suited for accumulation of multiple nitro groups and generation of polynitrated species, in particular of exhaustively substituted backbone combining two 3,5-dinitropyrazolyl groups. Energetic potency of such the dual could be estimated taking into account a simple prototype of 3,5-dinitropyrazole, which possesses higher heat effect of decomposition than that one for HMX.[16]

Results and discussion

Synthesis

Reactivity of the 4,4′-bipyrazole (**1**) supports special prospects for gradual nitro-functionalization, while all five nitration products (including two isomeric dinitro derivatives) may be prepared highly selectively and in excellent yields (Scheme 1). This reflects versatile behavior of the substrate, which is susceptible either to electrophilic substitutions or unconventional reactions in very dilute HNO_3 media, similar to reactions of phenol.[17] The latter case is illustrated by surprisingly ease mononitration of **1** in 1-5% acid, which presumably may

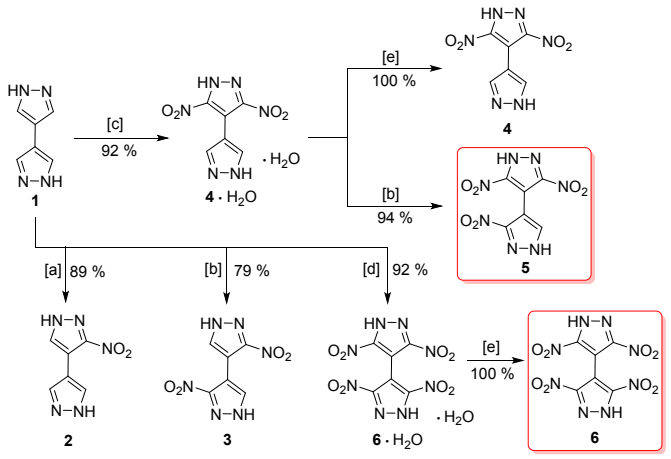

Scheme 1. Reaction pathways for selective nitro functionalization of the 4,4′-bipyrazole scaffold. Reagents and conditions: [a] 4% HNO_3, 95 °C, 6 h; [b] HNO_3, 82% H_3PO_4, 135 °C, 3 h; [c] 2.2 eq. HNO_3, 91% H_2SO_4, 100 °C, 3 h; [d] excess HNO_3, 91% H_2SO_4, 100 °C, 8 h; [e] 170 °C, 48 h.

not be associated with common electrophilic substitution. Under these conditions, pyrazole itself as well as 4-methyl- and 4-(pyridyl-4)-pyrazoles are completely inert giving corresponding nitrates only whereas similar 4,4′-bipyrazolium dinitrate was obtained by heating in concentrated acid.[18] With more drastic reaction conditions, such as heating at 140 °C in autoclave, further substitution occurs at the second pyrazole ring yielding symmetric 3,3′-dinitro-4,4′-bipyrazole (3). From preparative view, the latter reaction is more convenient in the media of 80% phosphoric acid, as high-boiling inert solvent. The observed selective mononitration of every pyrazole ring is strictly contrary to the behavior of 1 in the respect of typical electrophilic nitration in mixed acid. In this case, two pyrazole rings gradually undergo exhaustive *C*-nitration with the formation of 3,5-dinitro- (4) or 3,3′,5,5′-tetranitro-4,4′-bipyrazoles (6), depending on the ratio of the reagents. Selective dinitration at the same ring (compound 4), leaving the second ring unaffected, could be viewed as a chemical paradox, which is highly illustrative for general reactivity and protolytic properties of azoles. In fact, for the intermediate 2, the nitro group formally activates the carrier ring towards further substitution since nitration of the N-unsubstituted pyrazoles occurs on the conjugate acids[19] whereas weakly basic 3-nitropyrazoles undergo substitution as more reactive free bases. The normal deactivating (by over 8 log units) effect of nitro group was observed for 1,4-dimethylpyrazole nitrating as free base only.[20] When combined, the above selective mono- and dinitrations suggest a reliable two-stage reaction sequence toward the only remaining trinitroderivative 5. In this way, 1 is first converted to intermediate 4 and then to the desired 5 (94%) by successive nitrations in the media of H_2SO_4 and H_3PO_4, respectively. Compound 6·H_2O was previously mentioned in the conference proceedings without preparative details.[21] Our findings provide much wider versatility of the nitration reactions and the complete synthesis of the nitro derivatives 2–6 is shown in Scheme 1.

Single crystal X-ray diffraction studies

The solid-state structures of compounds **2**–**6** and **6**·H_2O were determined by XRD (Fig. 2). A particular example of **4** suggests that the basic pyrazole and appreciably acidic dinitropyrazole sites (pK_a = 3.14 for 3,5-dinitropyrazole[22]) are incompatible within the molecule and the latter exists rather as a peculiar pyrazolium/pyrazolate zwitter-ion.

Impact of progressive nitro substitution on molecular conformation of the bipyrazole core is best detected by gradual growth of the twist angle φ across the central C-C bond, as the number of nitro groups increases. Unlike exactly planar 4,4′-bipyrazole itself,[23] and nearly planar **2** [φ = 5.63(12)°], two isomeric dinitro compounds essentially lose coplanarity of two pyrazole halves and this effect is even more pronounced for **5** and **6** (Table 1).

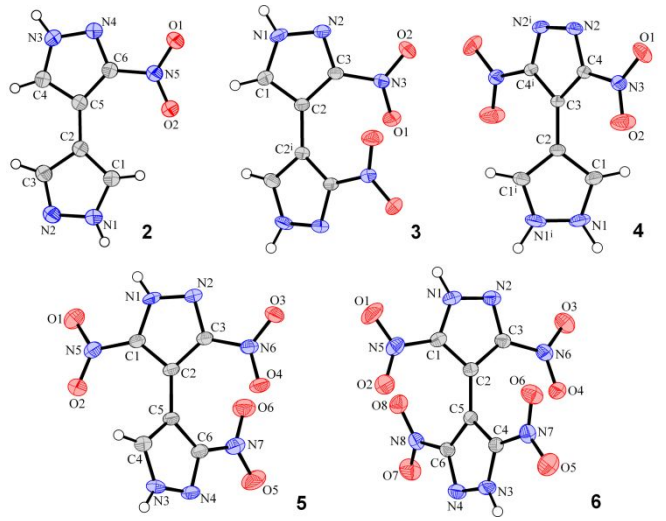

Fig 2. Molecular structures of **2–6** with atom labels and the thermal ellipsoids representing the 50% probability level.

Table 1. Selected parameters for structures of nitro 4,4′-bipyrazoles **2-6**

	NO_2 groups	Twist angle/° a)	Density/ g cm^{-3}	Packing index	H-bonded connectivity
1 [23]	0	0	1.424	69.9	Flat layer
2	1	5.63(12)	1.668	74.5	3D framework
3	2	46.48(4)	1.817	76.5	Flat layer
4	2	50.28(5)	1.836	76.6	Flat layer
5	3	58.58(9)	1.880	75.4	Corrugated layer
6	4	71.44(5)	1.847	72.2	Supramolecular tube
6·H_2O	4	78.99(6)	1.857	73.6	3D framework

a) The dihedral angle subtended by mean planes of two rings; for 4,4′-bipyrazole these rings were related by inversion.

However, the actual spread of twist angles for **3**–**6** is relatively small and the introduction of the third and fourth nitro groups does not provoke significant strains. Moreover, probably counterintuitive conformation of **3** (Fig. 2), which maintains short nitro-nitro stack [N···O = 3.019(14) Å], invokes certain attractiveness of intramolecular nitro-nitro interactions, as a special kind of π-hole/lone pair bonding.[24]

At the first glance, the twisted conformation of the molecules mitigates against dense molecular packings and thus the density of exhaustively nitrated **6** (1.847 g cm^{-3}) is even slightly less that of **5** (1.880 g cm^{-3}). However, a variety of supramolecular interactions in the structures contribute to the high packing indices [72.2-76.6%], at the upper limit of the 65–75% range expected for organic solids.[25] Pyrazole π-stacking is relevant only for pack of planar molecules of **2**, with two distinct H-bonded patterns segregating pyrazole or nitropyrazole sites within complicated 3D topology (further details can be found in the Supporting Information). It is worth noting that the conventional NH···N hydrogen bonds to nitropyrazole moiety commonly appear as bifurcated, with a second branch to the adjacent nitro-O acceptor [N···O = 2.8808(16)–3.1849(16) Å, for **2**–**6**] (Fig. 3). Evolution of supramolecular patterns, which coincides with progressive nitro substitution at the molecular frame, reflects increased role of nitro groups for H-bonding and π-hole/lone pair interactions.

Energetics and structural significance of the latter ones are comparable with weak CH···O bonding[24] and therefore the layered structures of **3**-**5** are very similar. In particular, the layers seen in the structure of **3** remain intact even with substitution at the third CH group thus yielding corrugated layers of **5** with short π-hole/lone pair NO_2/NO_2 stacks [N···O = 2.947(2) Å] instead of the CH···O bonds found in **3** (Fig. 3).

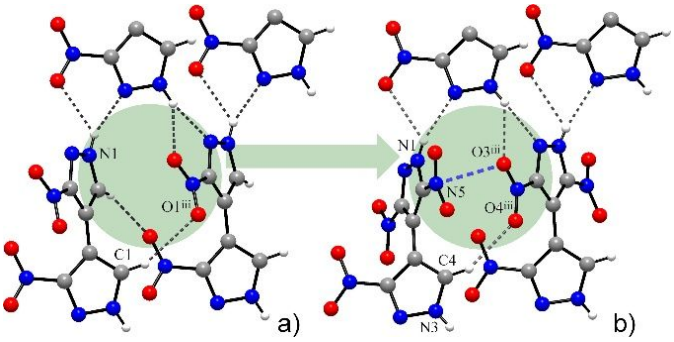

Fig 3. Inheritance of supramolecular motifs with increased number of nitro functionalities: the layers of **3** (a) and **5** (b) show comparable significance of CH···O and NO_2/NO_2 bonding [N5···O3^{iii} = 2.947(2) Å].

Effect of fourth nitro group is rather spectacular (**6**): with a larger twist angle imposed by the molecular frame and loss of interlayer CH···O linkage, the 2D array of H-bonded molecules collapses forming supramolecular tubes, *i.e.* one-periodic 2D structure (Fig. 4). The short NH···O bonds [2.8457(14) Å], generated in the replace of more common NH···N bonding, maintain tetramers of **6**, while bifurcate NH···O,N bonds extend the connectivity in one dimension. With a total elimination of competitive CH···O and stacking interactions, the role of nitro groups becomes crucial even beyond the hydrogen bonding: in total twelve short π-hole/lone pair N···O contacts (with a cut-off limit of 3.25 Å) of NO_2/NO_2 and NO_2/pyrazole types [shortest separations are 2.9115(15) and

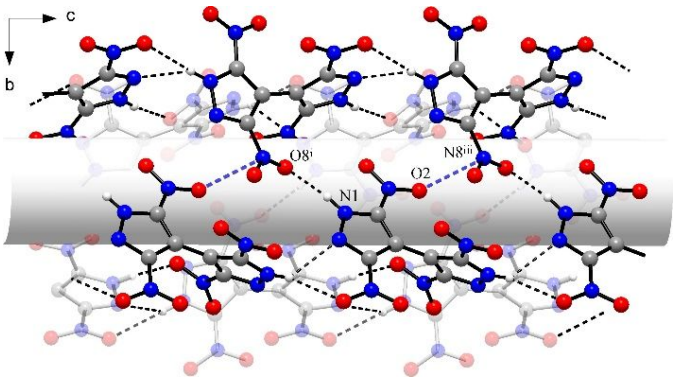

Fig 4. Structure of **6**: a supramolecular tube by interplay of hydrogen bonding and π-hole/lone pair interactions of nitro groups [N1···O8^{i} = 2.8457(14) Å; O2···N8^{iii} = 2.9115(15) Å].

Journal Name

ARTICLE

Table 2 Energetic properties and detonation parameters of compounds **2–6** compared to HNS

Compound	**2**	**3**	**4**	**5**	**6**	**6·H_2O**	**HNS**
IS[a] [J]	40	30	30	20	4.5	9	5
FS[b] [N]	>360	>360	>360	>360	192	324	240
ESD[c] [J]	0.74	0.63	0.54	0.50	0.30	0.40	0.80
Ω[d] [%]	−111.64	−71.38	−71.38	−44.58	−25.46	−24.08	−67.60
T_m[e] [°C]	284	377	284	306	292	292	–
T_{dec}[f] [°C]	303	382	302	314	298	298	318
ρ[g] [g cm^{-3}]	1.635	1.794	1.813	1.855	1.820	1.830	1.74
ΔH_f^{o}[h] [kJ mol^{-1}]	224.6	203.5	371.7	224.9	227.8	−11.0	78.2
EXPLO5 6.03							
$-\Delta_E U^{o}$[i] [kJ kg^{-1}]	3116.4	4036.4	4742.0	4821	5287	5039	5142
T_{C-J}[j] [K]	2367	3000	3357	3565	4054	3724	3677
p_{C-J}[k] [GPa]	14.4	22.1	24.9	28.6	31.1	30.7	24.3
D_{C-J}[l] [m s^{-1}]	6506	7528	7873	8256	8520	8451	7612
V[m] [dm^3 kg^{-1}]	481	436	430	417	419	418	602

[a] Impact sensitivity (BAM drophammer, method 1 of 6); [b] friction sensitivity (BAM drophammer, method 1 of 6); [c] electrostatic discharge device (OZM research); [d] oxygen balance; [e] melting point (DTA, β = 5°C·min^{-1}); [f] temperature of decomposition (DTA onset points, β = 5°C·min^{-1}); [g] density at 298 K; [h] standard molar enthalpy of formation; [i] detonation energy; [j] detonation temperature; [k] detonation pressure; [l] detonation velocity; [m] volume of detonation gases at standard temperature and pressure conditions.

2.8015(16) Å, respectively] contribute to the dense packing of this energetic material. These interactions approach the shortest reported contact of that type (2.80 Å) in the structure of the highly explosive heptanitrocubane[26] and they are relevant also for co-crystal 6·H_2O. Moreover, the water molecule also follows the trend by establishing its own π-hole/lone pair contact [N(nitro)···OH_2 = 3.058(2) Å], in addition to directional H-bonds and particularly strong NH···O bond [N···O = 2.6470(16) Å] with pyrazole (for further details on structure of 6·H_2O see the Supporting Information).

Physical and detonation properties

Since all synthesized nitro pyrazoles can be viewed either as important precursors for the synthesis of energetic materials (compounds **2**, **3** and **4**) or can be already classified as energetic materials (compounds **5** and **6**), their energetic behavior was investigated. All theoretically calculated and experimentally determined values for **2–6** compared to the thermally stable explosive HNS are listed in Table 2. Compound **6** ($T_{dec.}$ = 298 °C) decomposes slightly under 300 °C, whereas compounds **2** ($T_{dec.}$ = 303 °C), **3** ($T_{dec.}$ = 382 °C), **4** ($T_{dec.}$ = 302 °C) and **5** ($T_{dec.}$ = 314 °C) decompose above 300 °C. Although compounds **3** and **4** are structural isomers with only two NO_2 groups on the 4,4′-bipyrazole exoskeleton the difference in the decomposition temperature is significant. Increasing the number of NO_2 groups from three to four on the bipyrazole scaffold leads to only small decrease of the decomposition temperature from 314 °C to 298 °C for compounds **5** and **6**, respectively. All DTA and TGA plots for compounds **5** and **6** are depicted in the Supporting Information. The room temperature density values for compounds **5** and **6** are 1.855 g cm^{-3} and 1.820 g cm^{-3}, respectively. Experimentally determined sensitivity values toward impact and friction of **5** (IS = 20 J, FS = >360 N) exceed the reported values for PYX (IS = 10 J, FS = 360 N), HNS (IS = 5 J, FS = 240 N) and TKX-55 (IS = 5 J, FS = >360 N). Although the impact sensitivity of compound **6**·H_2O (IS = 9 J) is in the range of PYX (IS = 10 J), this value changes drastically for the anhydrous 6 (IS = 4.5 J). Figure 5 shows the change of the physico-chemical properties for the polynitrated pyrazoles **2–6** with increasing NO_2 groups in the 4,4′-bipyrazole scaffold.

For compounds **5** and **6** were estimated positive enthalpies of formation (**5** = 225 kJ mol^{-1} and **6** = 228 kJ mol^{-1}). Using these values, several detonation parameters for **2–6** were calculated (see the Supporting Information for details). The detonation pressure and velocity for **5** (p_{C-J} = 28.6 GPa, D_{C-J} = 8256 m s^{-1}) and **6** (p_{C-J} = 31.1 GPa, D_{C-J} = 8520 m s^{-1}) surpass the reported values for PYX (p_{C-J} = 25.1 GPa, D_{C-J} = 7757 m s^{-1}), HNS

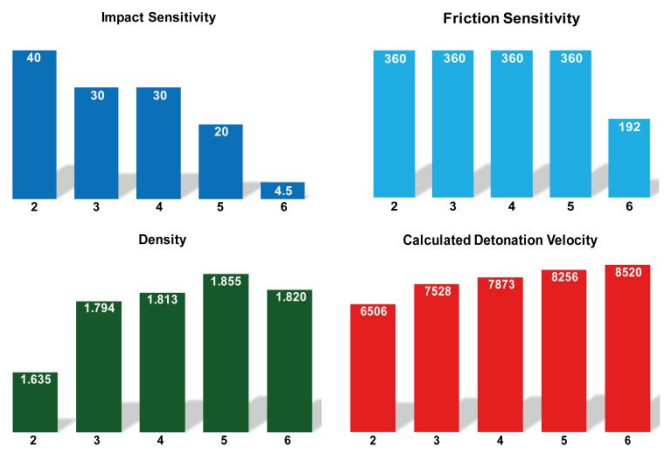

Fig 5. Bar charts for compounds **2–6** showing the change of the energetic behavior with increasing NO_2 groups in the 4,4′-bipyrazole scaffold. Impact Sensitivity [J], Friction Sensitivity [N], Density [g cm^{-3}] and Calculated Detonation Velocity [m s^{-1}].

($p_{C\text{-}J}$ = 24.3 GPa, $D_{C\text{-}J}$ = 7612 m s^{-1}) and TKX-55 ($p_{C\text{-}J}$ = 27.3 GPa, $D_{C\text{-}J}$ = 8020 m s^{-1}).[27]

In addition, the explosive performance of **5** and **6** on a small scale was investigated with the small scale shock reactivity test (SSRT, Fig. 6). The dent sizes were measured volumetrically by filling them with finely powdered SiO_2 and measuring the resulting weight. The obtained results for **5** and **6** are gathered in Table 3. The measured dent volume for **5** (640 mg) is in the range for the reported value for TKX-55 (641 mg) and slightly lower than the reported value for HNS (672 mg).[27] However, the solvent free **6** (811 mg) outperforms HNS, PYX and TKX-55 in the small scale shock test.

Table 3. The SSRT for **5** and **6** compared to HNS, PYX and TKX-55.

	HNS	PYX	TKX-55	**5**	**6**
m_E [mg][a]	469	474	496	500	491
m_{SiO2} [mg] [b]	672	637	641	640	811

[a] Mass of the explosive: $m_E = V_s \rho$ 0.95; [b] Mass of SiO_2.

Experimental

General Information

All reagents and solvents were used as received. The synthesis of 4,4′-bipyrazole **1** was performed by the previously published method.[23] Decomposition temperatures were measured *via* differential thermal analysis (DTA) with an OZM Research DTA 552-Ex instrument at a heating rate of 5 °C min^{-1} and in a range of room temperature to 400 °C and in addition thermal gravimetric analysis (TGA) of compounds **5**, **6** and **6**·H_2O was performed. The NMR spectra were recorded with a 400 MHz instrument (^{1}H 399.8 MHz, ^{13}C 100.5 MHz, ^{14}N 28.9 MHz, and ^{15}N 40.6 MHz) at ambient temperature. Chemical shifts are quoted in parts per million with respect to TMS (^{1}H, ^{13}C) and nitromethane (^{14}N, ^{15}N). Infrared spectra (IR) were recorded from 4500 cm^{-1} to 650 cm^{-1} on a Perkin Elmer Spectrum BX-59343 instrument with *Smiths Detection DuraSamplIR II Diamond ATR* sensor. The absorption bands are reported in wavenumbers (cm^{-1}). Raman spectra were recorded in glass tubes with Nd:YAG laser excitation up to 300 mW (at 1064 nm) in the range between 200 and 4000 cm^{-1}. The intensities are reported as percentages of the most intense peak and are given in parentheses. The sensitivities toward friction and impact of compounds **2-6** were determined according the BAM standards and the detonation parameters were calculated using the EXPLO5-V6.03 computer code.[28] All detonation parameters for the polynitro derivatives **2–6** were calculated by using the room-temperature densities obtained from the X-ray structures as described in the reference.[29] Compounds **2–6** and **6**·H_2O were tested for sensitivity towards electrical discharge using an Electric Spark Tester ESD 2010 EN.

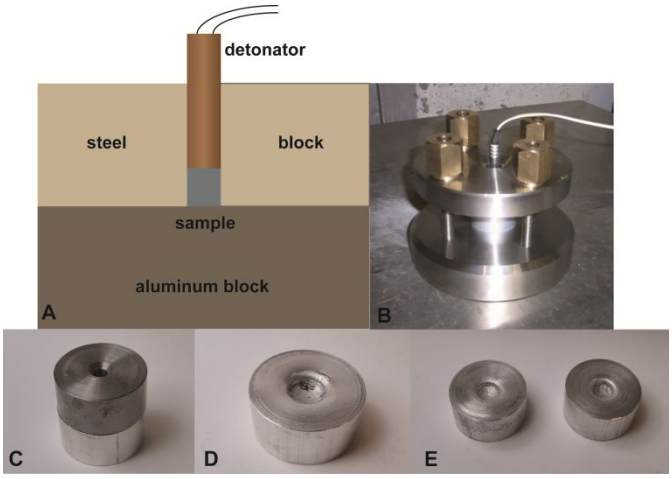

Fig 6. SSRT results for **5** and **6**; A) schematical illustration; B) photograph of the setup; C) aliminum block and steel block filled with the desired compound; D) dented aluminum block after initiation of compound **6** with a commercial detonator; E) dented aluminum blocks after initiation of compound **5** with a commercial detonator.

Crystallography

Single-crystal X-ray diffraction data were collected with graphite-monochromated Mo Kα radiation (λ = 0.71073 Å) using a Stoe Image Plate Diffraction System (φ oscillation scans). The structures were solved by direct methods and refined by full-matrix least-squares on F^2 using the programs SHELXS-97 and SHELXL-2014/7.[30] All hydrogen atoms were located and freely refined with isotropic thermal parameters. Crystallographic data for the reported structures in this contribution have been deposited with the Cambridge Crystallographic Data Centre as supplementary publication numbers (CCDC 1836403-1836408 for 2-6 and 6·H_2O). These data can be obtained free of charge from the Cambridge Crystallographic Data Centre via www.ccdc.cam.ac.uk/data_request/cif.

3-Nitro-4,4′-bipyrazole (**2**): 4,4′-Bipyrazole (**1**, 8.04 g, 60.0 mmol) was added to 4.5% aqueous solution of HNO_3 (820 mL, d = 1.023 g cm^{-3}; 0.6 mol) and the mixture was stirred at 95 °C for 6 h. The initially formed colorless crystalline deposit of 4,4′-bipyrazolium dinitrate dissolved for the first 30-40 min and during the next 2-3 h the mixture developed yellow color. The solution, while hot, was neutralized with 49.5 g (0.59 mol) of

solid $NaHCO_3$ and then cooled to r.t. Orange crystalline product (9.56 g, 89%) was filtered, washed with 20 mL water and dried on air. Pure material was obtained after recrystallization from hot water (3.5 g per 1 L).

2: Bright-orange platelets. DTA (5 °C min^{-1}): 256 °C (endo), 284 °C (melt.), 303 °C (exo.); BAM: drop hammer: 40 J (100–500 μm); friction tester: >360 N (100–500 μm); ESD: 0.74 J (100–500 μm). IR (ATR), $\tilde{\nu}$(cm^{-1}) = 3268 (m), 3233 (s), 3124 (m), 2923 (m), 2871 (m), 1698 (vw), 1609 (m), 1540 (w), 1502 (m), 1478 (w), 1406 (m), 1398 (m), 1334 (s), 1320 (s), 1297 (m), 1274 (m), 1241 (m), 1193 (m), 1208 (m), 1162 (m), 1106 (w), 1076 (m), 1034 (w), 960 (w), 943 (s), 877 (m), 851 (w), 829 (m), 796 (s), 762 (s), 649 (w), 640 (w), 614 (s), 504 (vw). Raman (1064 nm, 200 mW, 25 °C): $\tilde{\nu}$(cm^{-1}) = 3136 (4), 1614 (79), 1518 (18), 1409 (53), 1371 (5), 1341 (100), 1323 (3), 1301 (3), 1246 (5), 1223 (3), 1211 (5), 1164 (3), 1109 (3), 1085 (14), 929 (3), 831 (7), 506 (4), 400 (3), 222 (8). ^{1}H NMR (d_6-DMSO, 400 MHz, ppm) δ = 13.98 (s, 1H), 13.00 (s, 1H), 8.26 (s, 1H), 8.09 (s, 1H), 7.85 (s, 1H). ^{13}C NMR (d_6-DMSO, 101 MHz, ppm) δ = 151.7, 138.6, 130.3, 127.9, 109.9, 109.1. ^{14}N NMR (d_6-DMSO, 29 MHz, ppm) δ = −18. Anal. Calcd for $C_6H_5N_5O_2$: C 40.23, H 2.81, N 39.10 %. Found: C 40.21, H 2.75, N 38.80 %. *m/z* (DEI$^+$): 179.04 (4) [M]$^+$, 149.07 (32), 119.05 (31), 106.04 (20).

3,3′-Dinitro-4,4′-bipyrazole (**3**). **Method A**: 4,4′-Bipyrazole (**1**, 6.70 g, 50.0 mmol) and 35.0 mL (0.5 mol) of 65% nitric acid (d = 1.389 g cm^{-3}) were added to concentrated phosphoric acid (400 mL, 82%, d = 1.646 g cm^{-3}) held in 1 L round-bottom flask equipped with short air-cooled reflux condenser. The flask was placed into a pre-heated oil bath and the mixture was stirred at 130-135° C for 3 h. The mixture containing deposit of the reaction product was transferred onto 1.5 kg of crushed ice, the solid was filtered, washed with two portions of water and dried in air to yield compound 3 (8.85 g, 79%). The product was recrystallized from boiling water (0.4 g per 1 L) or, better, from 20% aqueous dimethylformamide (6.5 g per 1 L). **Method B**: 4,4′-Bipyrazole (**1**, 26.8 mg, 0.2 mmol), $Al(NO_3)_3{\cdot}9H_2O$ (93.8 mg, 0.25 mmol) and 15% HF (6 mL) were placed in a teflon-lined steel autoclave, heated at 140°C for 24 h and then cooled to r.t. over the period of 48 h. Large pale-yellow crystals of 3 (31.8 mg, 71%) were filtered, thoroughly washed with water and dried in air. The product is identical to the product of nitration by method A.

3: light yellow prisms. DTA (5 °C min^{-1}): 377 °C (melt.), 382 °C (exo.); BAM: drop hammer: 30 J (100–500 μm); friction tester: >360 N (100–500 μm); ESD: 0.63 J (100–500 μm). IR (ATR), $\tilde{\nu}$ (cm^{-1}) = 3198 (m), 3130 (m), 2960 (m), 1637 (vw), 1541 (w), 1532 (w), 1512 (m), 1482 (m), 1377 (s), 1351 (s), 1307 (m), 1246 (m), 1214 (m), 1140 (w), 1095 (m), 993 (m), 939 (w), 861 (w), 838 (m), 824 (s), 758 (s), 679 (w), 643 (s), 610 (w), 572 (m). Raman (1064 nm, 200 mW, 25 °C): $\tilde{\nu}$(cm^{-1}) = 1637 (49), 1551 (9), 1537 (13), 1496 (5), 1427 (3), 1398 (100), 1390 (13), 1377 (10), 1356 (26), 1308 (38), 1249 (6), 1209 (16), 1143 (8), 942 (19), 838 (17), 772 (6), 397 (6), 253 (7), 234 (18), 218 (7). ^{1}H NMR (d_6-DMSO, 400 MHz, ppm) δ = 14.13 (s, 2H), 8.20 (s, 2H). ^{13}C NMR (d_6-DMSO, 101 MHz, ppm) δ = 153.0, 132.5, 106.9. ^{14}N NMR (d_6-DMSO, 29 MHz, ppm) δ = −20. Anal. Calcd for $C_6H_4N_6O_4$: C 32.15, H 1.80, N 37.50 %. Found: C 32.10, H 1.94, N 37.35 %. *m/z* (DEI$^+$): 224.03 (99) [M]$^+$, 194.06 (41), 179.05 (47), 119.05 (100).

3,5-Dinitro-4,4′-bipyrazole (**4**): Fuming HNO_3 (5.65 mL, 98%, d = 1.501 g cm^{-3}) was added to a warm solution of **1** (8.04 g, 60 mmol) in 91% H_2SO_4 (240 mL, d = 1.820 g cm^{-3}). The mixture was placed into pre-heated oil bath and the clear solution was stirred at 100 °C (bath temperature) for 3 h. When cold, the mixture was poured into 0.5 kg of crushed ice giving clear pale-yellow solution. This was neutralized to pH = 4-5, with external ice cooling, by slow addition of concentrated ammonia (approximately 670 mL). The voluminous light-yellow precipitate of **4**·H_2O (13.36 g, 92%) was filtered and thoroughly washed with two 50 mL portions of ice water. Pure compound was obtained by recrystallization from boiling water (5.9 g per 1 L). The anhydrous material was obtained by recrystallization from ethanol.

4·H_2O: Light-yellow platelets. DTA (5 °C min^{-1}): 118 °C (H_2O, endo), 284 °C (melt.), 302 °C (exo.); IR (ATR), $\tilde{\nu}$(cm^{-1}) = 3578 (m), 3307 (w), 3142 (m), 2416 (m), 1806 (w), 1606 (w), 1523 (m), 1490 (s), 1401 (s), 1329 (s), 1241 (m), 1155 (m), 1097 (w), 1018 (w), 939 (m), 882 (s), 841 (s), 767 (m), 691 (w), 672 (vw), 619 (m), 560 (m). Raman (1064 nm, 200 mW, 25 °C): $\tilde{\nu}$ (cm^{-1}) = 3142 (6), 1611 (100), 1525 (17), 1495 (23), 1383 (92), 1299 (14), 1245 (14), 1214 (87), 1163 (6), 1112 (17), 941 (43), 822 (28), 761 (8), 674 (7), 404 (4), 384 (2), 374 (8), 335 (5), 283 (6), 264 (9). ^{1}H NMR (d_6-DMSO, 400 MHz, ppm) δ = 7.93 (s, 2H). ^{13}C NMR (d_6-DMSO, 101 MHz, ppm) δ = 148.2, 135.6 107.2, 104.5. ^{14}N NMR (d_6-DMSO, 29 MHz, ppm) δ = −24. Anal. Calcd for $C_6H_4N_6O_4{\cdot}H_2O$: C 29.76, H 2.50, N 34.71 %. Found: C 29.86, H 2.48, N 34.85 %. *m/z* (DEI$^+$): 224.03 (100) [M]$^+$, 194.06 (75), 105.03 (54).

4: Pale-yellow prisms. DTA (5 °C min^{-1}): 284 °C (melt.), 302 °C (exo.); BAM: drop hammer: 30 J (100–500 μm); friction tester: >360 N (100–500 μm); ESD: 0.54 J (100–500 μm). Anal. Calcd for $C_6H_4N_6O_4$: C 32.15, H 1.80, N 37.50 %. Found: C 32.03, H 1.90, N 37.49 %.

3,3′,5-Trinitro-4,4′-bipyrazole (5): Fuming HNO_3 (24.0 mL, 98%, d = 1.501 g cm^{-3}) was added to a slurry of **4**·H_2O (6.05 g, 25 mmol) in 82% H_3PO_4 (270 mL, d = 1.646 g cm^{-3}). The mixture was placed into pre-heated oil bath and the clear solution formed was stirred at 150°C (bath temperature) for 10 h. Precipitation of the reaction product was observed after first 5-6 h. The mixture was cooled, poured into 0.5 kg of crushed ice and left overnight at 5-10 °C. Pale-yellow deposit (5.64 g) was filtered and twice washed with 30 mL portions of water. Additional portion of the product (0.68 g) was isolated by extraction of the filtrates with EtOAc (3 × 300 mL). The combined yield was 6.32 g (94%). Pure **5** was obtained by crystallization from boiling water (8.0 g per 1 L).

5: Pale-yellow prisms. DTA (5 °C min^{-1}): 306 °C (melt.), 314 °C (exo.); BAM: drop hammer: 20 J (100–500 μm); friction tester: >360 N (100–500 μm); ESD: 0.50 J (100–500

μm). IR (ATR), $\tilde{\nu}$(cm^{-1}) = 3329 (m), 3156 (w), 3051 (w), 2801 (w), 1639 (w), 1549 (m), 1512 (m), 1478 (m), 1400 (s), 1334 (vs), 1298 (s), 1260 (m), 1228 (m), 1212 (m), 1167 (m), 1100 (m), 995 (m), 945 (w), 871 (w), 847 (s), 834 (s), 764 (m), 685 (vs), 629 (m), 604 (m), 587 (m), 546 (w), 518 (vw). Raman (1064 nm, 200 mW, 25 °C): $\tilde{\nu}$ (cm^{-1}) = 1640 (31), 1562 (5), 1544 (7), 1426 (11), 1399 (100), 1390 (13), 1340 (11), 1299 (5), 1265 (9), 1227 (6), 1210 (10), 947 (9), 833 (15), 754 (5), 519 (2), 360 (4), 316 (3), 270 (6), 237 (5), 209 (28). ^{1}H NMR (d_6-DMSO, 400 MHz, ppm) δ = 14.27 (br, 1H), 10.34 (br, 1H), 8.31 (s, 1H). ^{13}C NMR (d_6-DMSO, 101 MHz, ppm) δ = 153.2, 149.0, 134.4, 103.5, 102.6. ^{14}N NMR (d_6-DMSO, 29 MHz, ppm) δ = −24. ^{15}N NMR (d_6-DMSO, 41 MHz, ppm) δ = −20.3, −25.8, −82.8, −121.9, −170.5. Anal. Calcd for $C_6H_3N_6O_6$: C 26.78, H 1.12, N 36.43 %. Found: C 26.82, H 1.23, N 36.15 %. *m/z* (DEI$^+$): 269 (4) [M]$^+$, 239 (14), 223 (31), 93 (34), 77 (100).

3,3′,5,5′-Tetranitro-4,4′-bipyrazole (6): Fuming HNO_3 (43.7 mL, 98%, d = 1.501 g cm^{-3}) was added to a warm solution of **1** (8.04 g, 60 mmol) in 91% H_2SO_4 (350 mL, d = 1.820 g cm^{-3}). The mixture was placed into pre-heated oil bath and the clear solution formed was stirred at 98-100 °C (bath temperature) for 8 h. After cooling, the mixture containing colorless solid reaction product was poured into 1.2 kg of crushed ice and left overnight at 5-10 °C. Crystalline deposit of **6**·H_2O (18.32 g, 92%) was filtered, washed with 40 mL of ice water and dried. It was purified by crystallization from boiling water (45.0 g per 1 L). The compound crystallizes as monohydrate **6**·H_2O from a variety of wet solvents (alcohols, ethylacetate, aceton, 1,4-dioxane *etc*.). Anhydrous material **6** was obtained by crystallization from hot 1,2-dichlorobenzene (3.0 g per 1 L).

6·H_2O**:** Colorless prisms. DTA (5 °C min^{-1}): 115 °C (H_2O), 292 °C (melt.), 298 °C (exo.); BAM: drop hammer: 9 J (100–500 μm); friction tester: 324 N (100–500 μm); ESD: 0.40 J (100–500 μm). IR (ATR), $\tilde{\nu}$(cm^{-1}) = 3619 (w), 3520 (w), 3096 (w), 2954 (w), 2352 (w), 1844 (vw), 1574 (m), 1544 (s), 1512 (s), 1488 (s), 1421 (s), 1352 (s), 1329 (s), 1310 (s), 1288 (m), 1215 (m), 1198 (w), 1022 (m), 1004 (m), 951 (w), 839 (vs), 814 (m), 798 (m), 772 (m), 691 (m), 643 (vw), 613 (vw), 589 (vw), 514 (w). Raman (1064 nm, 200 mW, 25 °C): $\tilde{\nu}$ (cm^{-1}) = 1660 (7), 1565 (5), 1423 (4), 1400 (100), 1370 (4), 1313 (2), 1289 (2), 1226 (9), 1200 (2), 1007 (2), 829 (16), 756 (4), 590 (4), 374 (2), 269 (4). ^{1}H NMR (d_6-DMSO, 400 MHz, ppm) δ = 10.07 (s, 2H). ^{13}C NMR (d_6-DMSO, 101 MHz, ppm) δ = 149.7, 101.0. ^{14}N NMR (d_6-DMSO, 29 MHz, ppm) δ = −18. ^{15}N NMR (d_6-DMSO, 41 MHz, ppm) δ = −25.9, −114.8. Anal. Calcd for $C_6H_2N_8O_8$·H_2O: C 21.70, H 1.21, N 33.74 %. Found: C 21.89, H 1.46, N 33.57 %.

6: Colorless needles. DTA (5 °C min^{-1}): 292 °C (melt.), 298 °C (exo.); BAM: drop hammer: 4.5 J (100–500 μm); friction tester: 192 N (100–500 μm); ESD: 0.30 J (100–500 μm). IR (ATR), $\tilde{\nu}$ (cm^{-1}) = 3740 (vw), 3208 (m), 2967 (w), 1567 (s), 1519 (vs), 1482 (s), 1416 (s), 1348 (s), 1320 (vs), 1274 (w), 1207 (m), 1018 (w), 994 (m), 842 (vs), 758 (m), 744 (m), 712 (m), 675 (m), 635 (m), 580 (w), 518 (m). Anal. Calcd for $C_6H_2N_8O_8$: C 22.94, H 0.64, N 35.67 %. Found: C 23.04, H 0.85, N 35.66 %.

Conclusions

Our findings are important for a reliable approach towards facile accumulation of nitro functionalities at the pyrazole platform. *C*-nitrations at the 4,4′-bipyrazole (1), were performed under very simple, cost-effective and environmentally benign reaction conditions. The step-wize nitration causes a significant change increasing impact sensitivity and density and therefore energetic performance. Compounds 2–4 are especially promising intermediates, while exhibiting excellent thermal stability and low sensitivity towards external stimuli. Moreover, compounds 5 and 6 can be already classified as explosive materials showing excellent thermals stability and good sensitivities. Further functionalization of the 4,4′-bipyrazole scaffold is currently under investigation in our laboratories.

Conflicts of interest

There are no conflicts to declare.

Acknowledgements

Financial support of this work by the Ludwig-Maximilian University of Munich (LMU) and the Office of Naval Research (ONR) under grant no. ONR.N00014-16-1-2062 is gratefully acknowledged. We thank Dr. Burkhard Krumm for NMR measurements and Stefan Huber for his help with the sensitivity testing.

Notes and references

1 (*a*) H. Gao and J. M. Shreeve, *Chem. Rev.*, 2011, **111**, 7377; (*b*) T. M. Klapötke, *Chemistry of High-Energy Materials*, 3rd ed., De Gruyter, Berlin, 2015.
2 (*a*) T. Brinck (Ed.), *Green Energetic Materials*, John Wiley & Sons, 2014. (*b*) G. I. Sunahara, G. Lotufo, R. G. Kuperman and J. Hawari (Eds.), *Ecotoxicology of Explosives*, CRC Press, 2009.
3 (*a*) P. Yin and J. M. Shreeve, *Adv. Het. Chem.*, 2017, **121**, 89; (*b*) P. Yin, J. Zhang, C. He, D. A. Parrish, and J. M. Shreeve, *J. Mater. Chem. A*, 2014, **2**, 3200.
4 G. Hervé, C. Roussel and H. Graindorge, *Angew. Chem. Int. Ed.*, 2010, **49**, 3177.
5 (*a*) W.-Q. Tang, H. Ren, Q.-J. Jiao and W. Zheng, *Chin. J. Energ. Mat.*, 2017, **25**, 44; (*b*) S. Du, Y. Wang, L. Chen, W. Shi, F. Ren, Y. Li, J. Wang and D. Cao, *J. Mol. Model.*, 2012, **18**, 2105. (*c*) P. Ravi, D. M. Badgujar, G. M. Gore, S. P. Tewari and A. K. Sikder, *Propellants Explos. Pyrotech*. 2011, **36**, 393.
6 (*a*) D. Fischer, J. L. Gottfried, T. M. Klapötke, K. Karaghiosoff, J. Stierstorfer and T. G. Witkowski, *Angew. Chem. Int. Ed.*, 2016, **55**, 16132; (*b*) D. Kumar, G. H. Imler, D. A. Parrish and J. M. Shreeve, *J. Mater. Chem. A*, 2017, **5**, 10437; (*c*) D. Kumar, G. H. Imler, D. A. Parrish and J. M. Shreeve, *Chem. Eur. J.*, 2017, **23**, 7876; (*d*) P. Yin, J. Zhang, D. A. Parrish and J. M. Shreeve, *Chem. Eur. J.*, 2014, **20**, 16529.
7 (*a*) C. Li, L. Liang, K. Wang, C. Bian, J. Zhang and Z. Zhou, *J. Mat. Chem. A*, 2014, **2**, 18097; (*b*) Y. Tang, C. He, G. H. Imler, D. A. Parrish and J. M. Shreeve, *J. Mat. Chem. A*, 2018, **6**, 5136.
8 (*a*) Y. Tang, D. Kumar and J. M. Shreeve, *J. Am. Chem. Soc.*, 2017, **139**, 13684; (*b*) P. Yin, J. Zhang, G. H. Imler, D. A. Parrish and J. M. Shreeve, *Angew. Chem. Int. Ed.*, 2017, **56**,

8834; (*c*) P. Yin, C. He and J. M. Shreeve, *J. Mat. Chem. A*, 2016, **4**, 1514.
9 (*a*) P. Yin, D. A. Parrish and J. M. Shreeve, *J. Am. Chem. Soc.*, 2015, **137**, 4778; (*b*) Y. Zhang, Y. G. Huang, D. A. Parrish, and J. M. Shreeve, *J. Mater. Chem.*, 2011, **21**, 6891; (*c*) Y. Zhang, D. A. Parrish and J. M. Shreeve, *Chem. Eur. J.*, 2012, **18**, 987.
10 (*a*) P. Yin, L. A. Mitchell, D. A. Parrish and J. M. Shreeve, *Chem. Asian J.*, 2017, **12**, 378; (*b*) Y. Zhang, Y. Guo, Y. Joo, D. A. Parrish and J. M. Shreeve, *Chem. Eur. J.*, 2010, **16**, 10778.
11 (*a*) C. Li, M. Zhang, Q. Chen, Y. Li, H. Gao, W. Fu and Z. Zhou, *Chem. Eur. J.*, 2017, **23**, 1490; (*b*) J. Zhang and J. M. Shreeve, *Dalton Trans.*, 2016, **45**, 2363.
12 (*a*) J. C. Bennion, Z. R. Siddiqi and A. J. Matzger, *Chem. Commun.*, 2017, **53**, 6065; (*b*) J. Zhang and J. M. Shreeve, *CrystEngComm*, 2016, **18**, 6124.
13 S. F. Zhu, S. H. Zhang, R. J. Gou and F. D. Ren, *J. Mol. Model.*, 2018, 24:9.
14 L. Larina and V. Lopyrev, *Nitroazoles: synthesis, structure and applications*, Springer, Dordrecht, 2009.
15 J. W. A. M. Janssen, H. J. Kolners, G. G. Kruse and C. L. Habraken, *J. Org. Chem.*, 1973, **38**, 1777.
16 A. Bragin, A. Pivkina, N. Muravyev, K. Monogarov, O. Gryzlova, T. Shkineva and I. Dalinger, *Physics Procedia* 2015, **72**, 358.
17 J. H. Ridd, *Acta Chem. Scand.*, 1998, **52**, 11.
18 S. Trofimenko, *J. Org. Chem.*, 1964, **29**, 3046.
19 M. W. Austin, J. R. Blackborow, J. H. Ridd and B. V. Smith, *J. Chem. Soc.*, 1965, 1051.
20 A. R. Katritzky, H. O. Tarhan and B. Terem, *J. Chem. Soc. Perkin Trans. 2*, 1975, 1632.
21 I. L. Dalinger, T. K. Shkinyova, S. A. Shevelev, V. S. Kuz'min, E. A. Arnautove and T. S. Pivina, *Proceedings of the 29th International Annual Conference of ICT*, Karlsruhe, Germany, 1998, 57-1.
22 J. W. A. M. Janssen, C. C. Kruse, H. J. Koeners and C. L. Habraken, *J. Heterocycl. Chem.*, 1973, **10**, 1055.
23 I. Boldog, E. B. Rusanov, A. N. Chernega, J. Sieler and K. V. Domasevitch, *Angew. Chem. Int. Ed.*, 2001, **40**, 3435.
24 (*a*) A. Bauzá, T. J. Mooibroek and A. Frontera, *Chem. Commun.*, 2015, **51**, 1491; (*b*) A. Bauzá, A. V. Sharko, G. A. Senchyk, E. B. Rusanov, A. Frontera and K. V. Domasevitch, *CrystEngComm*, 2017, **19**, 1933.
25 J. D. Dunitz, *X-ray analysis and the structure of organic solids*, 2nd corrected reprint, 1995, Basel: Verlag Helvetica Chimica Acta, 106.
26 M.-X. Zhang, P. E. Eaton and R. Gilardi, *Angew. Chem. Int. Ed.*, 2000, **39**, 401.
27 T. M. Klapötke and T. G. Witkowski, *ChemPlusChem*, 2016, **81**, 357.
28 M. Sućeska, *EXPLO5 Version 6.03 User's Guide*, Zagreb, Croatia: OZM; 2015.
29 J. S. Murray and P. Politzer, *J. Mol. Model.*, 2014, **20**, 2223.
30 (*a*) G. M. Sheldrick, *Acta Crystallogr., Sect. A: Found. Crystallogr.,* 2008, **64**, 112. (*b*) G. M. Sheldrick, *Acta Crystallogr., Sect. C: Cryst. Struct. Commun.*, 2015, **71**, 3.

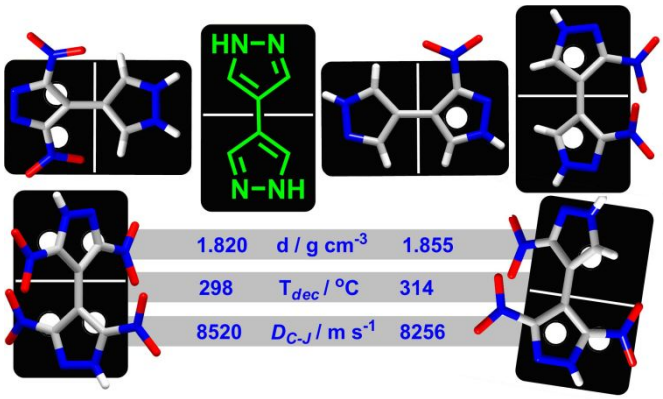

Graphical Abstract

Progressive nitro functionalization of 4,4'-bipyrazole yields insensitive and stable high explosives with excellent densities and detonation properties.